Astronomy Reports, Vol. 46, No. 4, 2002, pp. 327–338. Translated from Astronomicheskiĭ Zhurnal, Vol. 79, No. 4, 2002, pp. 364–376.

Origin of Prolonged X-Ray Flares on Active Late-Type Stars

I. M. Livshits and M. A. Livshits

Institute of Terrestrial Magnetism, Ionosphere, and Radio Wave Propagation, Russian Academy of Sciences, Troitsk, Moscow oblast, 142190 Russia

Received June 8, 2001

Abstract—Soft X-ray data for prolonged flares in subgiants in RS CVn binary systems and some other active late-type stars (AB Dor, Algol) are analyzed. During these nonstationary events, a large amount of hot plasma with temperatures exceeding 10^8 K exists for many hours. Numerical simulations of gas-dynamical processes in the X-ray source—giant loops—can yield reliable estimates of the plasma parameters and flare-source size. This confirms that such phenomena exist while considerable energy is supplied to the top part of a giant loop or system of loops. Refined estimates of the flare energy (up to 10^{37} erg) and scales contradict the widely accepted idea that prolonged X-ray flares are associated with the evolution of local magnetic fields. The energy of the current component of the large-scale magnetic field arising during the ejection of magnetic field by plasma jets or stellar wind is estimated. Two cases are considered: a global stellar field and fields connecting regions with oppositely directed unipolar magnetic fields. The inferred energy of the current component of the magnetic field associated with distortion of the initial MHD configuration is close to the total flare energy, suggesting that large-scale magnetic fields play an important role in prolonged flares. The flare process encompasses some portion of a streamer belt and may propagate along the entire magnetic equator of the star during the most powerful prolonged events.

1. INTRODUCTION. SOLAR–STELLAR ANALOGIES

Phenomena similar to solar activity develop on late-type stars that rotate and possess a surface convective zone. Impulsive flares in the optical continuum are observed fairly frequently on some red dwarfs. In recent years, stellar flares have been observed in soft X-rays, and both impulsive and prolonged nonstationary events lasting from several hours to 1–2 days have been detected. Flares with durations exceeding 3 h occur very seldom on dwarfs, whereas such events are observed fairly frequently on luminous, active late-type stars—in particular, some late-type subgiants in RS CVn systems, for which the energy of such flares exceeds the total energy of analogous phenomena on the Sun by four to five orders of magnitude.

In recent studies, it has usually been assumed that prolonged X-ray flares arise during the transformation of magnetic-field energy in the radiating volume to other kinds of energy, such as radiation, kinetic and thermal plasma energy, and energy of accelerated particles. A relationship similar to that usually applied to impulsive flares is used to estimate the energies of prolonged flares. The flare energy is taken to be the change in the energy of the local magnetic field in the region of primary energy release, which is at heights of less than 10 000 km in the case of impulsive solar flares.

The total energies of prolonged flares are estimated using the relationship

$$E_{\rm tot} = (B^2 - B_0^2)\frac{V_{\rm loop}}{8\pi}, \qquad (1)$$

where B and B_0 are the field intensities in the loop before and after the flare process and the volume $V_{\rm loop}$ is taken to be the loop volume. In (1), B_0 is determined from the condition that the magnetic and plasma pressures in the loop be equal at the flare maximum. This formula has been applied to the analysis of data for prolonged flares in a number of studies (see, for example, [1]). An exception is [2], in which the volume of the soft X-ray source in a flare is assumed to be comparable to the volume of the star and a different expression is used to estimate the energy. The intensities B for various prolonged flares estimated using (1) reach several kilogauss, which is completely implausible for fields in the coronae of the stars considered. This inconsistency stimulated our current study.

Below, we will use experience gained from analyses of X-ray data for solar flares. As a rule, impulsive flares develop at low heights, near the boundary between the chromospheric and coronal gas, in regions immediately adjacent to sunspots. The development of impulsive flares is connected in many respects with the acceleration of large numbers of electrons and with subsequent secondary processes, in particular,

1063-7729/02/4604-0327$22.00

the evaporation of hot plasma to the coronal part of the loop.

Frequently, a sufficiently powerful pulse will stimulate further development of the flare process. This is manifest as a brightening of many bright points along the line separating opposite polarities of the radial component of the magnetic field,[1] beginning from the site of the flare (frequently an "inlet" in the sunspot penumbra or even umbra) and sometimes extending to the boundaries of the active region. These bright points probably represent the feet of very low loops. The process moves upward over a few seconds, and a system of soft X-ray loops that gradual fill with hot plasma is ignited. An arcade of loops above a neutral line of the longitudinal magnetic field can radiate X-rays for up to an hour, with its feet being the brightest in both X-ray and optical lines during most of this time. In observations of the solar disk, these feet are visible as two ribbons, so such events are called two-ribbon flares. In addition to the feet, the region near the top is also bright in X-rays, visible as a cusp near the limb. In a large flare, there can be dozens of coronal loops (sometimes as many as several hundred), with the energy release being prolonged and strongly variable near the top of each. The "burning" of the loop arcade, which in most cases does not rise above 70 000 km, represents the basic process that we will call an active-region or X-ray flare.

One of the greatest achievements in solar-flare research was the detection and study of X-ray sources located near the tops of loops (or systems of loops). Observational evidence for magnetic reconnection as the primary source of energy release in prolonged flares [3, 4] was probably first obtained for the flare of February 21, 1992. An important unsolved problem is the role of coronal mass ejections (CMEs) in powerful, nonstationary processes. CMEs frequently begin near a flare maximum, with an eruption and rising of hot loops and divergence of the flare ribbons. Sometimes, eruptions of filaments (prominences)—i.e., cold plasma—can be observed instead of CMEs. The relationship between the onset of a two-ribbon flare and these eruptions has given rise to the name "eruptive flare" for these phenomena.

In connection with powerful stellar flares, we should point out two probable aspects of CMEs in the development of solar phenomena. First, a large-scale eruption can result in open magnetic configurations, at least at sufficiently great heights. This promotes the formation of a singular point of the magnetic field, probably at a height of about 0.1 $R_\odot$ from the surface in the case of large active regions. This creates the conditions necessary for reconnection (primary energy release). Further, the process must be supported over a time comparable to an hour.

The most powerful solar flares possess complex spatial and temporal structures. In many cases, a CME initiates another stage of a two-ribbon flare—ignition of the system in another part of the active region or activity complex; a well known example is the second flare observed on Bastille Day, July 14, 2000 [5]. This prolongs the overall duration of the event, sometimes by an appreciable factor, extending the process beyond the active region (to regions of weak magnetic fields) and facilitating the development of systems of giant arches (so-called dynamic flares in the terminology of Svestka *et al.* [6] and sigmoid-shape flares [7, 8]). In such phenomena, arches can rise to heights exceeding 100 000 km, and a system of giant arches can exist and be observable in both X-rays and H_α emission for up to a day.

Second, in the early 1980s, Sturrock [9] and Kopp and Pneuman [10] put forward the idea of posteruptive energy release. This suggests that a CME results in an open magnetic configuration and the appearance of additional currents in the corona. The system's recovery to the initial magnetic configuration may be accompanied by the formation of a vertical current sheet, with a possible subsequent reconnection of magnetic lines in this sheet.

Modern observations show that this idea is realized on the Sun during the recovery or formation of streamers [11] and also in processes leading to global restructuring of the corona [12]. Unfortunately, on the Sun, numerous CMEs are observed that are not accompanied by posteruptive energy release (i.e., significant X-ray flux); moreover, the X-ray radiation is weak in purely "coronal" solar flares, when this process is activated. Slow, high flares are most closely associated with CMEs, suggesting that the prolonged energy release is posteruptive in this case. In rare cases, these long-decay flares, which display a very prolonged decrease in their soft X-ray radiation, are adjacent to eruptions of systems of giant coronal loops, resulting in a global restructuring of the solar corona (see, for example, [12]). These phenomena occur outside the activity zone, at high latitudes, so formally they should not be considered flares.

However, a situation in which the large-scale magnetic field on the Sun is not sufficiently developed to provide the necessary efficiency of the associated posteruptive energy release is quite plausible. The situation may be different on active, late-type stars, especially those more luminous than the Sun. Therefore, the attractive model of Kopp and Pneuman [10] cannot be completely rejected when analyzing events on these stars.

[1] It is usual to call this the neutral line of the longitudinal magnetic field $H_{||}$.

The first explanation for prolonged emission from a nonstationary event in very soft X-rays (65–190 Å) on the red dwarf AU Mic was proposed by Cully *et al.* [13], who suggested that emission from a CME was detected in this event, which last more than half a day. In contrast, we proposed in [14] that such prolonged processes were associated with posteruptive energy release. We emphasize that the temperature in the source of very soft X-rays during the prolonged event on AU Mic was about an order of magnitude lower than at the maximum of the powerful prolonged stellar flares analyzed in the current paper.

In even a preliminary analysis of observations of prolonged stellar flares, the power and spectrum of their X-ray radiation suggest that dense loops with sizes comparable to the stellar radius may be the source of the emission. Therefore, when estimating the physical conditions in the radiating loops, it is useful to consider the energy balance in these loops. Based on studies of similar phenomena on the Sun [11, 15], we will consider the gas-dynamical stage of the process, when the magnetic field no longer appreciably affects the process, except for confining the plasma in the loop and maintaining the anisotropy of the heat transfer. This is consistent with the fact that the ratio of the gas and magnetic pressures, $\beta = 8\pi p/B^2$, begins to exceed unity at the large heights in the stellar coronae considered.

A large series of studies of variations of physical parameters during flares has been carried out on the basis of the one-dimensional Palermo–Harvard code for modeling gas-dynamical processes (see [16, 17] and references in [17]). This code was initially developed for short flares and has recently been applied to prolonged phenomena. The key point in this approach is taking into account the supply of material from the chromosphere to the coronal loop; for this reason, the calculations can successfully describe X-ray observations of flares lasting hundreds of seconds (see Fig. 4 in [17]).

However, in events lasting from many hours to several days, processes in the transition region between the chromospheric and coronal plasma no longer dominate, and the evolution of giant coronal loops becomes important. Accordingly, for prolonged events, we have computed the gas-dynamical processes in an already-formed coronal loop containing a fixed mass. The main aim of our simulations was to consider the energy balance in the loop and elucidate the major factors leading to such a slow decrease in the temperature during the process. We were also very interested in the relationship between the scale of the events and their power.

Below, we briefly discuss the main X-ray observations and a preliminary analysis of these observations, present the results of our simulations, and consider the question of the energy source for prolonged stellar flares.

2. X-RAY DATA ON PROLONGED STELLAR FLARES

Over the last ten years, observations of powerful flares on active late-type stars have been obtained by instruments on the Ginga, EUVE, ASCA, and BeppoSAX spacecraft. These observations were carried out in soft X-rays and the extreme ultraviolet. Most of these flares were on subgiants in RS CVn binary systems [18–20]; they include somewhat shorter events, for example, on the young, late-type G star AB Dor [1], as well as prolonged processes on Algol—a B8 IV–V + G–K IV binary [21]. Some prolonged soft X-ray and EUV flares were detected for the red dwarfs AU Mic and EV Lac. Some observational data and the results of an analysis of the soft X-ray radiation from prolonged stellar flares are listed in the table.

The table shows that the plasma temperature at the maximum of many long-duration flares exceeds 100 MK and that the high temperatures and emission measures persist for many hours. Prolonged flares on the subgiant UX Ari occur fairly frequently for RS CVn stars. In particular, on August 29, 1994, ASCA observed the growth phase and maximum of a flare with maximum temperature $T_{\max} = 220$ MK and emission measure $\mathrm{EM} = 3 \times 10^{54}$ cm^{-3} [2]. On November 9, 20, and 22, 1995, three flares with durations for the X-ray decay phase of 5.2, 23.0, and

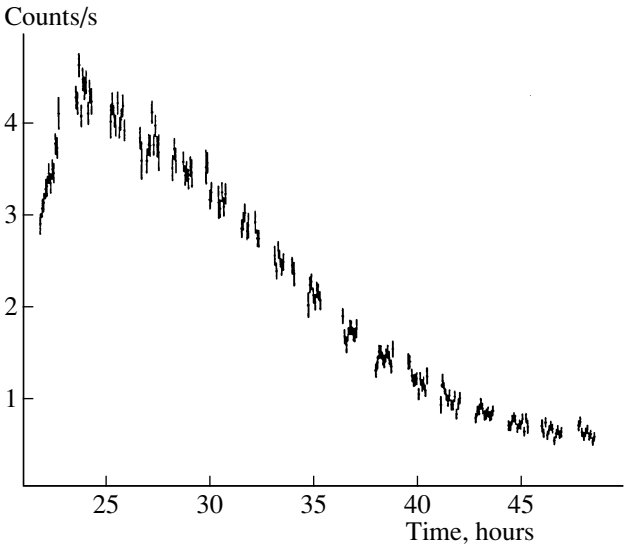

Fig. 1. A sample recording of the X-ray emission from a prolonged stellar flare. This flare on UX Ari was observed on August 28–30, 1997, on BeppoSAX in the 1.8–10.5-keV range by Pallavicini and Tagliaferri [19].

Data on prolonged X-ray flares

Date	Star	T, 10^6 K	EM, 10^{54} cm^{-3}	t, h	E_X, erg	Spacecraft	Reference
July 24–25, 1987	UX Ari	>100	10	>12	10^{37}	Ginga	[22]
August 28–30, 1997	UX Ari	111.5	5.13	30	5×10^{36}	BeppoSAX	[19]
November 9, 1997	AB Dor	110	5.5	5	4×10^{35}	BeppoSAX	[1]
November 29, 1997	AB Dor	110	3.7	4	7×10^{35}	BeppoSAX	[1]
August 30, 1997	Algol	≈100	10	50	1.4×10^{37}	BeppoSAX	[21]
June 23–25, 1991	HR 5110	110	0.7	70	$>4 \times 10^{36}$	ROSAT	[20]

31.5 h were observed during long-term monitoring with EUVE [18]. Note that the interval from November 19–25, 1995, can be considered a single, prolonged nonstationary event on this star.

Hard emission with $h\nu > 20$ keV was recorded from one of the most powerful flares on UX Ari on August 29, 1997 [19], giving rise to appreciable interest in the processes occurring on this star. BeppoSAX recorded $T = 111.5$ MK and EM $= 5.13 \times 10^{54}$ cm^{-3} for this hard X-ray flare, which lasted longer than a day, on August 28–30, 1997 (Fig. 1), during the time of the maximum observed soft X-ray flux. Note that the total energy of this flare was comparable to that observed for this star by Ginga [22] in a flare that lasted about a day. Pallavicini and Taglioferri [19] believe that the total energy of the flare of August 28–30, 1997, exceeded 6×10^{36} erg.

3. RESULTS OF NUMERICAL SIMULATIONS OF THE EVOLUTION OF GIANT FLARE LOOPS

Let us briefly consider the general problem of modeling prolonged X-ray flares on the Sun and active late-type stars. It is known that the soft X-ray emission from impulsive events on the Sun and stars is connected with the free radiation of a hot coronal cloud (loop) formed during the flare. Following Pallavicini *et al.* [23], we introduce the time scale for the decline in the count rate or luminosity of the X-ray radiation by a factor of e, $\tau_d = d \ln I/dt$. In impulsive flares, τ_d is determined by the plasma radiative time scale in the source, $\tau_{\rm rad} = 3kT/nL(T)$, where, as usual, $L(T)$ is the volume radiative-loss function; the radiative losses are usually taken to be $n_e^2 L(T)$ for a unit volume. For prolonged flares, τ_d exceeds $\tau_{\rm rad}$ by a factor of 3–30, distinguishing these events from impulsive phenomena and requiring additional plasma heating in the source of the soft X-ray radiation.

To estimate the energy required for the flare process and the plasma parameters in the source, we will consider, as in [5], a simple one-dimensional model for the behavior of a fixed amount of plasma in a loop with a constant cross section. For simplicity, we will take the loop axis to be semicirclular (Fig. 2). As the gas in the top part of the loop is heated, the loop can either expand or contract.

We analyzed the energy balance in a single giant loop by solving a set of one-dimensional gas-dynamical equations taking into account the height variations of the gravity, heat conduction, and radiative losses:

$$\frac{\partial v}{\partial t} = -\frac{\partial p}{\partial s} - g, \qquad (2)$$

$$\frac{\partial z}{\partial s} = \frac{1}{n m_{\rm p}},$$

$$\frac{\partial \varepsilon}{\partial t} = -p\frac{\partial v}{\partial s} - \frac{\partial W}{\partial s} - Q_{\rm rad} + H.$$

Here, the Lagrangian coordinate s and Euler coordinate z (along the loop) are measured from the base of the corona of the quiescent star, the Lagrangian coordinate $s(z) = \int_{z_0}^{z} n(z') m_{\rm p} dz'$, $n = n_e = n_{\rm p}$ is the density of completely ionized hydrogen plasma, $m_{\rm p}$ is the proton mass, the thermodynamic equations of state for such plasma are $p = 2nkT$ and $\varepsilon = 3kT/m_{\rm p}$, g is the gravitational acceleration, $W = -\kappa m_{\rm p} n \frac{\partial T}{\partial s}$ is the heat flux, $\kappa = 10^{-6} T^{5/2}$ is the heat conductivity, $Q_{\rm rad} = (1/m_{\rm p}) n L(T)$ are the radiative losses, and H is the heating of the plasma per unit mass.

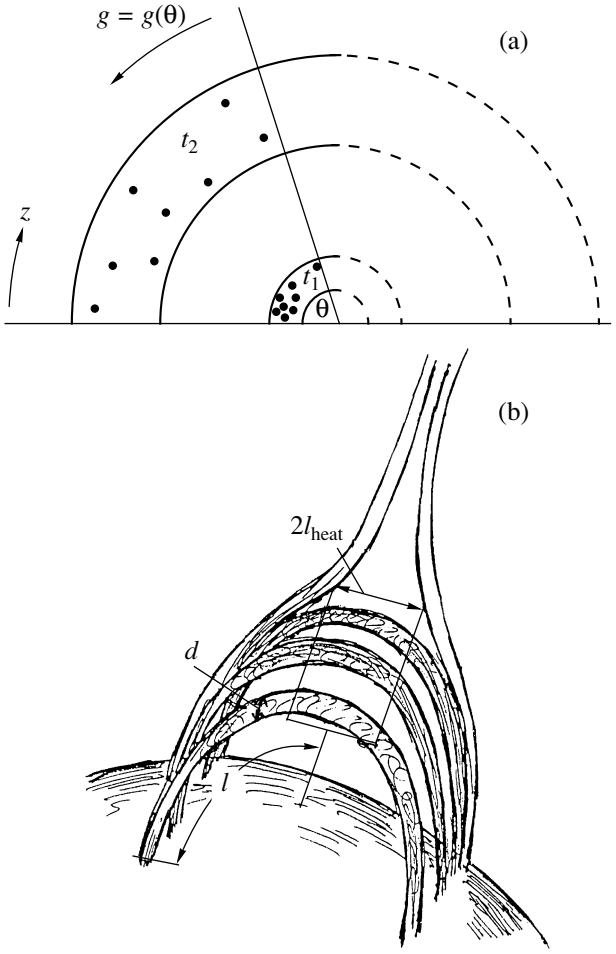

Fig. 2. (a) Schematic presentation of a loop for two times. The gravity depends on the position angle, i.e., the height in the corona. (b) Schematic of a system of loops; d is the loop diameter, $2l$ its length, and $2l_{\rm heat}$ the total size of the heated region (in Section 4 , the extent of the entire system along the neutral line of the magnetic field is designated ζ).

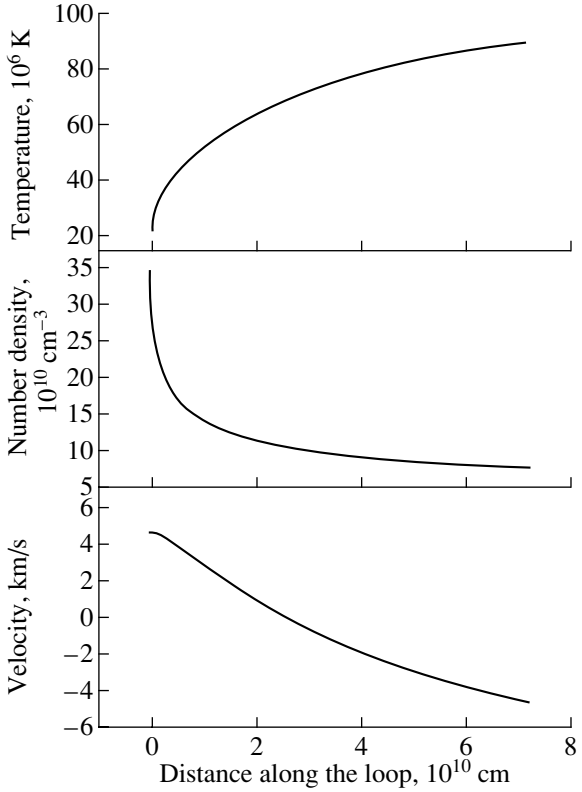

Fig. 3. Variation of physical parameters along the loop 5 h after the onset of the flare on UX Ari. The distance along the loop is measured from one of its feet. Positive velocities correspond to plasma motion away from the photosphere (i.e., the loop is contracting).

The gas mass is specified by the density at the feet of a loop with constant temperature. The boundary conditions are constancy of the pressure at the loop extremes and, for the energy part of the system, constancy of the temperature from below and of the thermal flux from above (specifically, we have accepted $dT/dl = 0$). These initial conditions correspond to an isothermal hydrostatic loop with some density at its feet, temperature ($T > 10^6$ K), and loop (half-)length. Thus, the choice of the mass of heated gas is also determined.

The development of the process essentially depends on the heating. As earlier, we assumed that plasma heating takes place near the loop top and is distributed in time and in space (over the mass Lagrangian coordinate):

$$H = H_0 \cdot \exp\left\{-\left(\frac{s}{s_1}\right)^2\right\} \cdot \exp\left\{-\left(\frac{t-t_1}{t_2}\right)^2\right\}, \quad (3)$$

where H_0 is the amplitude in erg g^{-1} s^{-1}, t_1 is the time to achieve the maximum, and t_2 is the width of the temporal profile.

In order for the process considered to be possible—i.e., for the bottom part of the loop to not cool before the arrival of the heat perturbation—we introduced a small constant contribution to the heating function, numerically equal to the radiative energy losses of the corona outside the flare. This stationary heating did not exceed 10% of H_0 for the flares simulated here. Note that the effect of this heating is also manifest in the final stage of the event, at the end of the main heating.

Our modification of the earlier code [15], developed for solar flares, makes it possible to perform computations for various values of the gravitational acceleration and other characteristic parameters. In particular, the radiative-loss function was extended

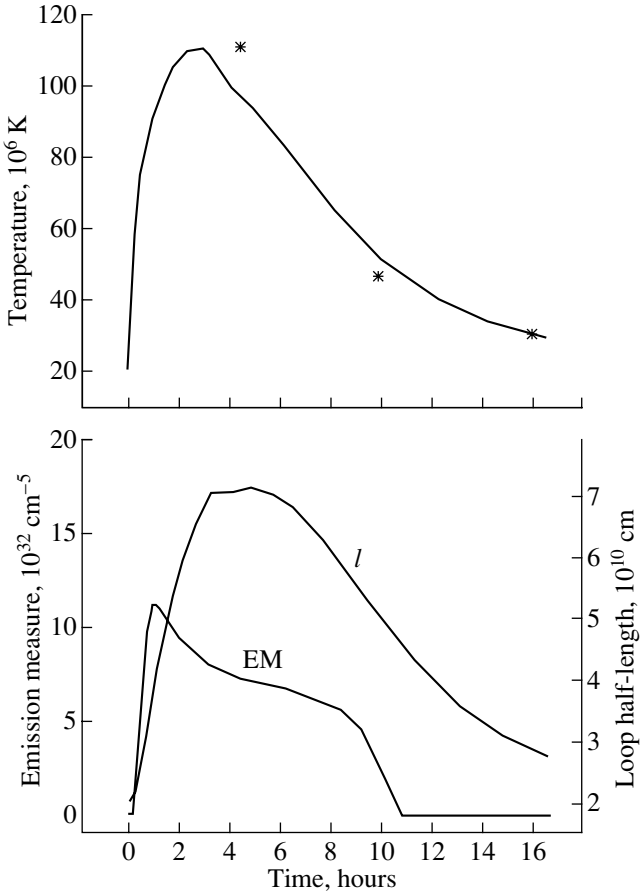

Fig. 4. Results of modeling the flare on UX Ari: time dependences for the temperature at the loop top, emission measure, and loop half-length. The observed temperatures from [19] are shown with asterisks.

compared to the treatment in [15] to temperatures $T > 20$ MK, in accordance with the calculations of [24]: $L(T) = 10^{-24.73}T^{0.25}$ cm^3 s^{-1}.

We note here two points.

(1) We use the boundary condition at the loop feet, allowing the loop to expand in both directions. To model flares in active regions on the Sun (the hot phases of solar flares), the best condition at the loop feet is $v = 0$, which implicitly takes into account some input of plasma from the chromosphere to the coronal part of the loop. This formulation of the problem is closer to [17], which leads to better consistency of the solutions.

(2) Generally speaking, the code is intended primarily for simulations of the decay phase. Computations for the entire flare lead to difficulties due to the asymmetry of the growth and decay phases in the soft X-ray light curve observed in the overwhelming majority of cases. The evolution of a giant coronal loop with smooth, slowly varying heating characteristically shows similar durations for loop expansion and contraction phases, accompanied by radiative growth and decay. When modeling the observed growth phase for the X-ray radiation, which lasts only 0.5–1 h in the events analyzed, large plasma velocities in the loop result. After the loop expansion is replaced by contraction, the downward plasma motions lead to the formation of shocks near the loop feet, making further computations impossible. To model the next, very prolonged, decay phase of processes developing in the densest loops, we must either dampen these motions artificially or make computations for the growth and decay phases separately when modeling powerful events. The final results of these two artificial approaches do not differ strongly.

We carried out simulations for initial densities at the feet of an isothermal loop from 2×10^{10} to 5×10^{11} cm^{-3}, sizes for the loop half-length $l = (0.5–5) \times 10^{10}$ cm, and heat fluxes varying over broad limits. We considered processes whose total energy did not exceed 10^{37} erg. We obtained temperatures at the loop top in the range (10–200) MK. The gravitational acceleration could take on values 10^2–4×10^4 cm s^{-2}.

When modeling processes for a particular star, there was some set of parameters for which a small

change of one or more of them led to a change in the character of the process and a transition from weak to strong expansion of the loop. These two classes of solutions existed in virtually all the examples we analyzed. In the computations for powerful processes in dense loops, these two classes of solutions also differed in that the temperature at the event maximum was either below or above 100 MK.

We carried out simulations for three late-type stars, which, together with the Sun, cover the main types of active objects on which prolonged X-ray flares have been observed. The first was the K0 subgiant in the UX Ari binary system, where analogous activity is very strongly pronounced. The gravitational acceleration for this star is rather small: we adopted $g_* = 8.8 \times 10^2$ cm/s^2. The second star, AB Dor, is the well-known young K1 dwarf, with an age of only 20–30 millions of years; as in [1], we adopted the stellar radius $R_* = R_\odot$, mass 0.76 $M_\odot$, and, accordingly, $g_* = 2.14 \times 10^4$ cm/s^2. As an example of prolonged X-ray superflares, which are observed in Algol and RS CVn systems, we have considered a giant flare on HR 5110≡BH CVn (F2IV+K2IV) [20], assuming the mass ratio for this system to be $M_2/M_1 = 0.54$ and the gravitational acceleration on the secondary K subgiant to be $g = 4 \times 10^3$ cm/s^2.

We paid special attention to the simulations for UX Ari. Figures 3 and 4 show the results of the computations for this star with $H_0 = 4.5 \times 10^{13}$ erg/(g s), $t_1 = 0.5$ h, and $t_2 = 5$ h. This strong heating can supply the observed temperature in an X-ray flare. The initial density at the feet of the isothermal loop with $T_0 = 20$ MK was $n_0 = 4 \times 10^{11}$ cm^{-3}, and the loop half-length was $l = 2 \times 10^{10}$ cm.

Figure 3 shows a typical distribution of physical parameters along the loop for the onset of the decay of an X-ray flare (5 h after the beginning of the flare process). The temperature profile reflects the fact that heat conduction is the main process for heat transfer. The density decreases with height, but exceeds 7×10^{10} cm^{-3}, even at very large heights. The velocities of the loop expansion or contraction (i.e., of the plasma motions near the loop feet) are several km/s, which is typical of our simulations. Note that the loop size has increased over the initial size by a factor of 3.5.

Figure 4 shows the distribution of temperature at the loop top, the emission measure of the hot gas with $T > 50$ MK, and the loop half-length during the flare. Three observed temperatures referred to the centers of the exposures are also given. We can see that in the flare decay phase the process considered can cool the X-ray source over a half day. The emission measures of the plasma with temperature $T > 50$ MK are given here for one half of the loop, EM_l (maximum 10^{33} cm^{-5}); we obtain the value $\mathrm{EM}_V = 5 \times 10^{54}$ cm^{-3} for the entire system of loops by multiplying the calculated values of EM_l by the "effective" area 5×10^{21} cm^2 (see below). Thus, the existence of a hot source over about half a day can be explained.

The asymmetry of the $T(t)$ dependence in Fig. 4 is due to the assumed time behavior for the main heating, and the temperature decrement is almost completely determined by the value of t_2. At the latest stage of the flare, heating from the surrounding corona becomes important, affecting the shape of the $T(t)$ curve.

Note that the temperature behavior outstrips the variations in the loop length. The time for the maximum loop expansion virtually coincides with the time when the highest temperature is achieved, but the temperature then falls, with any appreciable contraction occurring only after some delay. In this giant flare, the sharp contraction of the loop after the peak of the nonstationary event (sometimes observed on the Sun—the so-called "shrinkage" effect [4]) is almost invisible. In this case, the absence of this feature is due to very intense heating under low-gravity conditions.

Powerful but shorter flares can also be successfully analyzed using these simulations. In particular, Figure 5 shows similar results for a typical X-ray flare on AB Dor. The initial conditions in the loop were similar to those used previously—$T_0 = 20$ MK and $n_0 = 4 \times 10^{11}$ cm^{-3}—but the initial loop half-length was somewhat smaller, $l = 1.5 \times 10^{10}$ cm. The main difference from the previous case is the heating-function parameters at the loop top ($H_0 = 1.5 \times 10^{13}$ erg/(g s), $t_1 = 6.7$ min, $t_2 = 1$ h), as well as the shorter (by approximately a factor of four) duration of the event (see Fig. 4). This also affected the loop half-length, which was about two-thirds that for the flare on UX Ari. Note that, for subsequent comparison with the observations, Figure 5 shows the emission measure of gas with $T > 30$ MK rather than $T > 50$ MK, as in Fig. 4; therefore, the actual emission measures for the two cases are similar.

We were also able to model the superflare on HR 5110. However, the result turned out to be similar to that already discussed above for UX Ari. A description of the entire process requires a somewhat slower decay of the heating function. The loop half-length is slightly greater than $l = 8 \times 10^{10}$ cm. The question of whether the whole set of flare activity on UX Ari on November 19–25, 1995 [18], should be considered a single flare or a superposition of series of bursts remains open. The shape of the light curve of the flare on HR 5110 is better described by a single flare event. A transition to greater heating fluxes results in the ejection of a system of loops. The

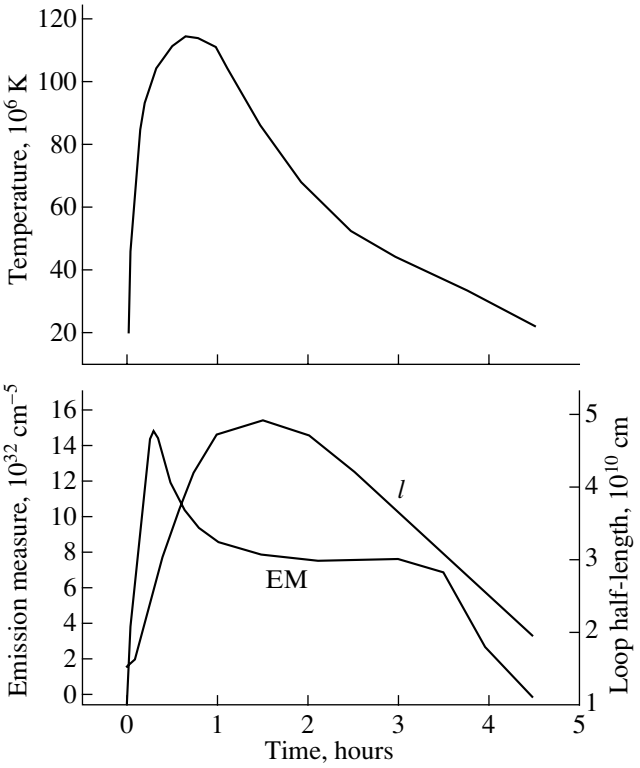

Fig. 5. Same as in Fig. 4 for a typical prolonged X-ray flare on AB Dor.

flare on Algol g [21] has similar parameters as that on HR 5110, and simulations also proved possible.

Our simulations enable us to estimate the area of the flares projected onto an image of the corona (i.e., onto the celestial sphere). Let us assume that the flare center consists of a set of m loops, each with a length $2l$ (Fig. 2b). In this case, the volume emission measure can be represented

$$\mathrm{EM}_V = S_1 \mathrm{EM}_l = 2md^2 \int_0^l n_e^2 dl, \qquad (4)$$

where d is the loop diameter. The value of EM_V is obtained from observations, while $\mathrm{EM}_l = \int_0^l n_e^2 dl$ is yielded by the simulations.

The total energy of the process is

$$E = S_2 H_f = 2ml_{\mathrm{heat}}\, d \iint H\, ds dt, \qquad (5)$$

where l_{heat} is the length of the heated part of the loop. During its operation, the code computes the total heating, i.e., integrated over the Lagrangian coordinate s and over time: $H_f = \iint H\, ds\, dt$ (in units of erg cm^{-2}).

For example, for the flare on UX Ari we have considered, $H_f \approx 6.2 \times 10^{14}$ erg cm^{-2} and $\mathrm{EM}_l \approx 7 \times 10^{32}$ cm^{-5} throughout the decay phase, which lasted 14 h. From the values in the table, $E = 5 \times 10^{36}$ erg and $\mathrm{EM} = 5.1 \times 10^{54}$ cm^{-3}, we obtain $S_1 \approx S_2 = 8 \times 10^{21}$ cm^2. Accordingly, for the flare on AB Dor, $H_f \approx 1.3 \times 10^{14}$ erg cm^{-2} and $\mathrm{EM}_l \approx 7 \times 10^{32}$ cm^{-5} during the decay phase, which lasted about 4 h. From the values $E = 5 \times 10^{35}$ erg and $\mathrm{EM} = 5 \times 10^{54}$ cm^{-3}, we obtain $S_1 \approx 4 \times 10^{21}$ cm^2 and $S_2 \approx 7 \times 10^{21}$ cm^2. We can see that, for these two powerful flares with very different durations, the areas of the X-ray source were very large. This implies that a prolonged flare can indeed be considered to represent the evolution of stationary loops that diverge with height. Such ideas were developed in [25]. The difference between the S_1 values for the two flares testifies to their different L_{heat}/d ratios. Essentially, we can use the two above equations to estimate the number of loops m and diameter of each loop d. We can say only that our analysis favors a large number of thin loops; however, the accuracy of these estimates is low.

For the entire sample of prolonged X-ray flares considered, ranging from those occurring on the Sun, on red dwarf stars, and weak events on subgiants to powerful events on active late-type stars, our analysis leads us to conclude that flare power is to some extent related to the size of the coronal loop but very

strongly depends on the extent of the corresponding loop system along the neutral line of the magnetic field. In any case, prolonged heating of the plasma at appreciable heights in the loops is required for such flares to develop.

4. ESTIMATE OF THE TOTAL MAGNETIC-FIELD ENERGY

The energies of the prolonged stellar flares we are studying are very large. They would require, for example, the annihilation of oppositely directed magnetic fields with intensities of $(1-2)\times 10^3$ G in the entire volume of the system of giant loops ($V \approx \mathrm{EM}_V/n^2 \approx 10^{31}-10^{32}$ cm^3). Fields this strong cannot exist in the outer atmospheric layers of the stars considered, in particular, in their lower coronae. Therefore, reconnection of local magnetic fields cannot supply the energy required by these flares.

Attention was first drawn to the fact that some stellar activity may be related to the evolution of larger scale (not local) magnetic fields in [26]. For nonstationary processes, this refers first and foremost to prolonged posteruptive energy release resulting in the development of systems of giant coronal loops. We can imagine the reconnection of lines of force in the equatorial region of the global (dipole) field of the entire star, deformed by the stellar wind. For the Sun, this corresponds to the streamer belt, located above the region where the interplanetary current sheet adjoins the corona.

Let us estimate the energy of the current component of the magnetic field for the entire streamer belt around a star. We will use the stationary solution of the following problem [27]. We set a dipole magnetic field on a sphere of radius R, which stretches outward to a medium with a given magnetic Reynolds number Re_m. The stationary solution of the basic equation of ideal magnetic hydrodynamics with the boundary condition for the radial magnetic field component $B_r\big|_{r=R} = 2m\cos\theta/R^3$ on a sphere of radius R was sought in [27] as

$$B_r = \frac{1}{r^2}\frac{1}{\sin\theta}\frac{\partial\psi}{\partial\theta}, \tag{6}$$

$$B_\theta = -\frac{1}{\sin\theta}\frac{\partial\psi}{\partial\theta}. \tag{7}$$

Separating variables, we obtained in [27] the solution

$$\psi = \frac{a\sin^2\theta}{R(\mathrm{Re}_m+2)}\left(\mathrm{Re}_m + 2\frac{R}{r}\right). \tag{8}$$

The run of the field lines for $\mathrm{Re}_m = 10$ is shown in Fig. 7 in [27].

Integrating over the volume outside the sphere of radius R, we obtain the energy of this field:

$$E = 2\frac{m^2}{3\,R^3}\left(1 - \frac{2\,\mathrm{Re}_m + 2}{(\mathrm{Re}_m+2)^2}\right) \approx 2\frac{m^2}{3\,R^3}. \tag{9}$$

Taking into account the fact that the energy of the corresponding dipole magnetic field outside the sphere of radius R is

$$E = \frac{m^2}{3\,R^3} \tag{10}$$

(see, for example, [28]), we find that, for large Reynolds numbers, the energy of the current components is close to the energy of the dipole field.

We can estimate the energy stored in a heliospheric current sheet as follows. At the solar minimum, the global solar magnetic field is close to dipolar, with the dipole axis close to the rotational axis. At large distances from the Sun, the lines of force of the interplanetary magnetic field are nearly radial. The simplest way the sources of such a field can be represented in the outer corona and distant parts of the heliosphere is as a superposition of a point-like dipole for the Sun and an infinitely thin ring current in the equatorial plane with surface current density $j_\phi \sim r^{-3}$ [29]. Tarasova *et al.* [30] estimated that the energy stored in this current is of the order of the dipole field energy contained above the onset of the wind outflow. This is consistent with the results of our integration of the distribution of a field with the form depicted in Fig. 2 in [27].

The previous relationship can be rewritten $E = (1/3)B_\odot^2 R_\odot^3$. With a field near the solar poles $B_\odot = 1$ G, we obtain a current energy of 1.1×10^{32} erg. Note that performing the integration starting from the sphere of the solar wind source does not substantially change this value. The estimated energy does not exceed the energy of prolonged solar flares.

Dipole-type magnetic fields on active late-type stars are now beginning to be measured, and the derived intensities are of the order of tens of gauss (see, for example, [31]). The stellar wind from active late-type stars, especially subgiants in RS CVn systems, is much more powerful than the solar wind. For UX Ari, whose K0 subgiant has a radius of $4.7R_\odot$ and a field on the dipole axis of 30 G, the estimated current energy is $E \approx 3\times 10^{36}$ erg. The sizes of some other active late-type stars are not so large, but, in general, the fields can be somewhat stronger.

We emphasize that a prolonged stellar flare need not encompass the entire streamer belt. Most often, the flare process occurs in some interval of longitudes along the neutral line of the large-scale field. Observations of large, nonstationary events on the Sun show that two cases are possible. In the first,

the neutral line is frequently distorted and the surface of the interplanetary current sheet becomes nonplanar and corrugated. This occurs if unipolar regions with oppositely directed magnetic fields develop on opposite sides of the neutral line of the large-scale field. This corresponds to a four-sector structure of the interplanetary magnetic field, which most often exists in the heliosphere. Nonstationary processes that develop as stability is disrupted in some part of the streamer belt result in a global restructuring of the corona.

In the second case, from time to time during a cycle, large activity complexes form in the same longitude interval, in which powerful X-ray flares lasting from several hours to about a day can occur. This case is the closest to the prolonged stellar flares considered in this paper. The energy of such events can be estimated by approximating the magnetic field by that of a plane dipole, as is sometimes done for two-ribbon flares on the Sun. Here, we will present a very simple estimate, though it will be necessary to consider this problem in more detail as new results concerning the large-scale magnetic fields of stars become available.

Let us direct the z axis along the neutral line. We then have for the magnetic field of a horizontal dipole at some depth beneath the photosphere (see, for example, [32]):

$$H = \left\{ \frac{2\mu xy}{(x^2+y^2)^2}, \quad \frac{\mu(y^2-x^2)}{(x^2+y^2)^2}, \quad 0 \right\}. \quad (11)$$

Here, generally speaking, the magnetic moment of the dipole μ can depend on time. The lines of force lie in the xy plane and are circles centered on the x axis and passing through the coordinate origin. We will assume that the x axis is directed radially and that the y axis is parallel to the photosphere at the position of the active region considered. Introducing the quantity $\rho = (x^2+y^2)^{1/2}$, we readily obtain a relationship for the field energy in the region $\rho \geq \rho_1$:

$$E = \frac{\Delta z}{8\pi}\int H^2\, ds = \frac{\zeta}{8\pi}\int \frac{\mu^2}{\rho^4}\, 2\pi\rho\, d\rho = \frac{\mu^2\zeta}{8\rho_1^2}, \quad (12)$$

where $\zeta \equiv \Delta z$ is the extent of the arch system along the z axis.

The magnetic moment μ is related to the field intensity: when $y = 0$, $H_y = -\mu/\zeta^2$, with $x = \zeta$ at the loop top. The field energy in the region $\rho \geq \rho_1$ for $\rho_1 = 1/3\ \zeta$ is then estimated as

$$E = (9/8)H_y^2\zeta^3. \quad (13)$$

Thus, the estimated magnetic-field energy in a plane-dipole approximation does not differ very strongly from the case of a global dipole, with the natural distinction that this energy depends on the extent of the system of loops along the neutral line. The distortion of the magnetic field of a plane dipole by a stellar wind is known [32], and the meaning of that problem is close to that demonstrated in [27] for a star as a whole. Repeating the analysis carried out at the beginning of this section for a global dipole, we find that the current energy arising from a distortion of the magnetic field of a plane dipole agrees with (13) to within a few tens of percent. This indicates that for the magnetic field the energies of prolonged X-ray stellar flares can be estimated using (13).

For giant arch systems in solar activity complexes, we can adopt $\zeta = 10^{10}$ cm (that is, $1/7R_\odot$ and less than 0.1 of the radius of the stars considered) and $H_y = 10$ G at the top of the loops. Then, (13) corresponds to $E \leq 10^{32}$ erg, in agreement with observations of solar flares. On some active late-type stars, the field strengths and sizes can exceed those typical of the solar corona by an order of magnitude. In particular, the field intensity in activity complexes on stars or in two oppositely directed unipolar regions can appreciably exceed the field intensity near the poles (tens of gauss), as indicated by data on variations of the intensities of global fields on some late-type stars. Therefore, flares with total powers up to 10^{37} erg are possible on the most active late-type stars, as was recently observed.

5. CONCLUSION

We have analyzed recent data on the physical conditions in the sources of soft X-ray emission in prolonged flares on active late-type stars. The appearance of a large amount of plasma heated to temperatures from 50 to 100 MK is due to flare processes in giant coronal loops. By modeling the gas-dynamic processes in such a loop heated from above, we have estimated the physical conditions in the sources of soft X-ray emission for both weak flares and the most powerful prolonged flares on active late-type stars.

Our calculations confirm the results of computations using the one-dimensional Palermo–Harvard gas-dynamical code, which indicate that such flares last as long as the necessary heating continues in the top part of the loop. Furthermore, both approaches show that heat transfer dominates over other dissipative processes, in particular, radiative losses in the bulk of the loop so that the time behavior of the temperature in the source of soft X-ray emission reflects variations in the heating.

In contrast to [17], we did not use any additional assumptions, such as the conservation of entropy or adoption of a similarity law for the physical conditions in the loop. This enabled us to more reliably determine the plasma parameters and the flare-source

size. We found that powerful heating can last from several hours to a day or more, with the plasma density in a coronal flare source exceeding 10^{11} cm^{-3}. Further development of these studies requires multiwavelength observations making it possible to directly estimate the densities in flare arches on active late-type stars.

Strong, prolonged flares differ from similar weaker events in the size of the loops involved and the extent of the system of loops along the neutral line of the magnetic field. The flare process occupies a part of the streamer belt, possibly propagating along the entire magnetic equator during the most powerful prolonged phenomena.

Our calculations can be used to estimate the total energy necessary to realize each event. The total energy of such flares, which can reach 10^{37} erg, rules out the possibility that prolonged stellar flares are associated with the evolution of local magnetic fields, widely accepted in earlier studies.

We have estimated the energy of the current component of the large-scale magnetic field, which results from the ejection of lines of force by plasma outflows or stellar wind. We have considered two cases: a global stellar field and fields connecting regions with oppositely directed unipolar magnetic fields. The estimated energy of the magnetic-field current component associated with a distortion of the initial MHD configuration is close to the total soft X-ray energy from prolonged flares and also to values yielded by our gas-dynamical simulations. Therefore, it is quite natural to associate the origin of prolonged flare phenomena with the reconnection of large-scale magnetic fields, particularly in the immediate vicinity of the tops of giant coronal loops.

Note that the weak prolonged phenomena sometimes observed on typical flare stars (both red dwarfs and late-type subgiants), characterized by fairly low plasma temperatures at the loop tops (< 10 MK), may be associated with a purely posteruptive energy release localized in vertical current sheets at large distances from the stellar surface [14].

A comparison of prolonged X-ray events on red dwarfs (and the Sun) and active subgiants suggests that, in addition to their scale, these phenomena differ in the role of coronal mass ejections in their general nonstationary processes. In the events we have analyzed here, the main role of each CME is initiating new flare centers along the neutral line of the large-scale magnetic field. On the Sun, this type of flare process is observed much more rarely [5] than the evolution of dynamic flares—rising systems of giant arches with posteruptive energy release.

The development of the most powerful processes under conditions of relatively low gravity should result in disruption of the system of loops and the ejection of plasma. Therefore, there is every reason to believe that some fraction of the energy of prolonged superflares is directly transferred to nonstationary processes developing even in the space between the components of binary systems. Our analysis of superflares supports this possibility, suggested earlier for flares on HR 5110 [20].

ACKNOWLEDGMENTS

The authors are grateful to S.I. Plachinda and I.S. Veselovskiĭ for useful discussions. This work was supported by the Russian Foundation for Basic Research, project nos. 99-02-16289 and 01-02-17693.

REFERENCES

1. A. Maggio, R. Pallavicini, F. Reale, and G. Tagliaferri, Astron. Astrophys. **356**, 627 (2000).
2. M. Güdel, J. L. Linsky, A. Brown, and F. Nagase, Astrophys. J. **511**, 405 (1999).
3. S. Tsuneta, Astrophys. J. **456**, 840 (1996).
4. T. G. Forbes and L. W. Acton, Astrophys. J. **459**, 330 (1996).
5. I. M. Chertok, V. V. Fomichev, A. A. Gnezdilov, and R. Gorgutsa, Sol. Phys. (2001) (in press).
6. Z. Svestka, F. Farnik, H. S. Hudson, *et al.*, Sol. Phys. **161**, 331 (1995).
7. R. C. Canfield, H. S. Hudson, and D. E. McKenzie, Geophys. Res. Lett. **26**, 627 (1999).
8. H. Wang, P. R. Good, C. Dencera, *et al.*, Astrophys. J. **536**, 971 (2000).
9. P. A. Sturrock, Nature **211**, 695 (1966).
10. R. A. Kopp and G. W. Pneuman, Sol. Phys. **50**, 85 (1976).
11. K. V. Getman and M. A. Livshits, Astron. Zh. **76**, 704 (1999) [Astron. Rep. **43**, 615 (1999)].
12. A. McAllister, M. Dryer, P. McIntosh, and H. Singer, J. Geophys. Res. **101** (A6), 13497 (1996).
13. S. L. Cully, G. Fisher, M. J. Abbott, and O. H. W. Siegmund, Astrophys. J. **435**, 449 (1994).
14. M. M. Katsova, J. Drake, and M. A. Livshits, Astrophys. J. **510**, 986 (1999).
15. K. V. Getman and M. A. Livshits, Astron. Zh. **77**, 295 (2000) [Astron. Rep. **44**, 255 (2000)].
16. G. Peres, R. Rosner, S. Serio, and G. S. Vaiana, Astrophys. J. **252**, 791 (1982).
17. R. M. Betta, G. Peres, F. Reale, and S. Serio, Astron. Astrophys., Suppl. Ser. **122**, 585 (1997).
18. R. Osten and A. Brown, Astrophys. J. **515**, 746 (1999).
19. R. Pallavicini and G. Tagliaferri, Palermo Astronomy Preprint No. 4 (1998).
20. V. G. Graffagnino, D. Wonnacott, and S. Schaeidt, Mon. Not. R. Astron. Soc. **275**, 129 (1995).
21. F. Favata, J. H. M. M. Schmitt, G. Micela, *et al.*, Astron. Astrophys. **362**, 628 (2000).
22. T. Tsuru, K. Makishima, and T. Ohashi, Publ. Astron. Soc. Jpn. **41**, 679 (1989).

23. R. Pallavicini, G. Tagliaferri, and L. Stella, Astron. Astrophys. **228**, 403 (1990).
24. R. Mewe, J. S. Kaastra, and D. A. Liedahl, Legacy **6**, 16 (1995).
25. G. H. J. Van Den Oord and F. Zuccarello, in *Stellar Surface Structure,* Ed. by K. G. Strassmeier and J. Linsky (Kluwer, Dordrecht, 1996), p. 433.
26. M. M. Katsova and M. A. Livshits, in *Proceedings of the 11th Cambridge Workshop on Cool Stars, Stellar Systems and the Sun, 2001,* Ed. by R. J. G. Lopes, R. Rebolo, and M. R. Z. Osorio; Astron. Soc. Pac. **223**, 979 (2001).
27. S. Kouchmy and M. A. Livshits, Space Sci. Rev. **61**, 393 (1992).
28. F. A. Ermakov, *Physics of Solar Activity* [in Russian], Ed. by E. I. Mogilevskiĭ (Nauka, Moscow, 1988), p. 25.
29. I. S. Veselovskiĭ, Geomagn. Aeron. **34** (6), 1 (1996).
30. I. S. Veselovsky, in *Proceedings of the 9th European Meeting on Solar Physics, Magnetic Fields and Solar Processes, Florence, 1999,* ESA SP-448, p. 1217.
31. T. N. Tarasova, S. I. Plachinda, and V. V. Rumyantsev, Astron. Zh. **78**, 550 (2001) [Astron. Rep. **45**, 475 (2001)].
32. B. V. Somov and S. I. Syrovatskiĭ, in *Neutral Current Layers in Plasma* [in Russian] (Nauka, Moscow, 1974), Tr. Fiz. Inst. Akad. Nauk SSSR, Vol. 74, p. 14.

Translated by G. Rudnitskiĭ